Catalysis Today 241 (2015) 8–14

Contents lists available at ScienceDirect

Catalysis Today

journal homepage: www.elsevier.com/locate/cattod

Surface fluorination on TiO_2 catalyst induced by photodegradation of perfluorooctanoic acid

Sara Gatto[a,c], Maurizio Sansotera[b,c,*], Federico Persico[b,c], Massimo Gola[b,c], Carlo Pirola[a,c], Walter Panzeri[d], Walter Navarrini[b,c], Claudia L. Bianchi[a,c]

[a] Dipartimento di Chimica, Università degli Studi di Milano, Via Golgi 19, 20133 Milano, Italy
[b] Dipartimento di Chimica, Materiali e Ingegneria Chimica "Giulio Natta", Politecnico di Milano, Via Mancinelli 7, 20131 Milano, Italy
[c] Consorzio Interuniversitario Nazionale per la Scienza e Tecnologia dei Materiali (INSTM), Via G. Giusti 9, 50121 Firenze, Italy
[d] C.N.R.—Consiglio Nazionale delle Ricerche, Istituto di Chimica del Riconoscimento Molecolare, "U.O.S. Milano Politecnico", Via Mancinelli 7, 20131 Milano, Italy

ARTICLE INFO

Article history:
Received 20 January 2014
Received in revised form 1 April 2014
Accepted 28 April 2014
Available online 2 July 2014

Keywords:
Titanium dioxide
PFOA
Photocatalysis
Pollution
HPLC–MS
^{19}F-NMR

ABSTRACT

The photoabatement of perfluorooctanoic acid in aqueous solution has been performed with a commercial nano-sized TiO_2-based photocatalyst content of 0.66 g/L under an UV irradiation of 95 W/m^2. PFOA degradation intermediates were investigated by HPLC–MS and ^{19}F-NMR analysis. Evidences of a degradation mechanism based on two competitive pathways are discussed: photo-redox and β-scission pathways. Shorter perfluorinated carboxylic acids, $C_nF_{2n+1}COOH$ (n = 1–6), as expected degradation intermediates, were identified and their concentration trends over time were determined. The apparent pseudo-first order kinetic constant expressed as rate of PFOA disappearance was also measured: k_{app} 0.1296 h^{-1}. The influence of fluoride ions on TiO_2 surface was analyzed by XPS technique, revealing a surface modification that affects the performances of the catalyst.

1. Introduction

Perfluorooctanoic acid (PFOA), $C_8HF_{15}O_2$ (AMW = 414.07 g/mol), a representative of perfluorinated chemicals (PFCs), is largely used as surfactant in the fluoropolymers synthesis with the aim to obtain chemical compounds with specific properties for a wide range of industrial applications, such as manufacturing, aerospace, automotive, electronics, semiconductors and textile [1,2]. Moreover, PFOA is applied for the production of breathable membranes for clothing, e.g. Gore-Tex® [3]. Its strong stability and high surface-active effects are due to the presence of C—F bonds (about 130 kcal/mol) in its molecular structure [4,5].

However, many studies indicate that PFOA is environmentally persistent and bioaccumulative [6,7]. For these reasons, in the last years many research groups have devoted efforts to develop methods able to eliminate PFOA from the environment [8,9]. Actually, the US-EPA (Environmental Protection Agency) and EEA (European Environmental Agency) launched an industrial program aimed to reduce global emissions and product content of PFOA and related chemicals. In agreement with these directives, the eight major producers of fluoropolymers and fluorotelomers have been coerced into reducing global facility emissions and product content of PFOA and its related chemicals by 95% in 2010 as well as to completely eliminate emissions and product content of PFOA by 2015 [10,11].

Many procedures have been developed over the years for the removal of surfactants from water [12]. Traditional techniques include air stripping, biological processes, incineration and chemical treatments, but each method presents some negative aspect limiting its industrial feasibility [13,14]. For example, biological processes cannot reach a complete degradation of the pollutant and incineration can produce fully persistent and toxic by-products [12].

Therefore, besides classical wastewater treatment techniques, in the last decades advanced oxidation processes (AOPs) have increasingly become a valuable alternative [15–17]. In such processes, very reactive hydroxyl radicals are generated and, thanks to their high redox potential (E_0 = 2.73 V), they are responsible for the oxidation of organic pollutants [18–20]. AOPs methods can be distinguished on the basis of the oxidizing agent source involved in photolysis, photocatalysis, ultrasound, microwave or

* Corresponding author at: Politecnico di Milano, Dipartimento di Chimica, Materiali e Ingegneria Chimica "Giulio Natta", Via Mancinelli 7, 20131 Milano, Italy. Tel.: +39 02 2399 3035; fax: +39 02 2399 3180.
E-mail address: maurizio.sansotera@polimi.it (M. Sansotera).

http://dx.doi.org/10.1016/j.cattod.2014.04.031
0920-5861/

ozone treatments and Fenton processes. Among these, we adopted photocatalysis based on a semiconductor in combination with UV light and oxygen. Many studies have been carried out using titanium dioxide for the degradation of organic pollutants in both water and air phase [21,22]. TiO_2 is characterized by chemical and biological inertness, high photocatalytic activity, photodurability, mechanical robustness and relative cheapness. Therefore, these features offer great potential, especially for industrial scale water treatment.

The present paper is focused on PFOA photodegradation promoted by commercial TiO_2 powder (P25 by Evonik®). The mineralization was monitored by total organic carbon (TOC) analysis and ionic chromatography (IC) and the intermediate degradation products were determined by high-performance liquid chromatography combined with mass spectrometry (HPLC–MS) analysis. The presence of the fluorinated surfactant in solution was also monitored by ^{19}F-NMR. HPLC–MS and ^{19}F-NMR analyses were performed on samples of PFOA solution collected from the photoreactor after different reaction times. The degradation and changes in the fluorinated solution during the process were assessed by these techniques highly endowed to reveal the structure changes of molecules that could take place in the reaction environment. Finally, XPS analysis allowed the evaluation of chemical modifications occurring on the surface of the photocatalyst powder.

2. Materials and methods

2.1. Materials

Perfluorooctanoic acid (purity 96%—from Sigma Aldrich®) was used as received. PFOA is soluble in water (9.5 g/L) and its critical micelle concentration (CMC) is 7.80×10^{-3} mol/L at 25 °C [6]. Titanium dioxide P25 (75% Anatase, 25% Rutile [23]) was supplied by Evonik® and it was tested as titanium-based photocatalyst. Water was purified using an Elga Option 3 deionizer and was used to prepare all solutions. Milli-Q water was employed for ion chromatography. HPLC–MS analyses were carried out using as eluting phase a mixture of methanol (CHROMASOLV®, for HPLC, ≥99.9%—from Sigma Aldrich®) and 2 mM aqueous ammonium acetate solution.

2.2. Photocatalysis

The photocatalytic apparatus was a 1-L glass stirred reactor equipped with an iron halogenide UV lamp (500 W, Jelosil® HG500) emitting light at wavelengths of 315–400 nm and able to irradiate the reactor with a specific power of 95 W/m^2. The UV lamp was placed beside the reactor, which was cooled with water at a temperature of 30 ± 0.5 °C [24]. Titanium dioxide was introduced in the reactor at the beginning of each test (0.66 g/L). As previously reported, the variation of the surfactant concentration in solution was monitored by total organic carbon (TOC) analysis and ionic chromatography [24]. The PFOA initial concentration ($[PFOA]_0$ = 4 mM) was maintained lower than its CMC (7.8 mM) in order to avoid the formation of emulsions during the kinetic tests. Thus, the PFOA initial concentration was high enough to allow the detection also of the degradation intermediates at low concentrations. Samples (10 mL) of the reaction mixture were collected at different reaction times: typically at 0 min (before the start of the reaction), 30 min, 1 h, 2 h, 3 h, 4 h, 6 h and 9 h. Each kinetic test was repeated three times in order to evaluate the error extent. Each sample was centrifuged and filtered through a 0.45 μm polycarbonate membrane in order to separate the TiO_2 powder from the solution. The residual photocatalytic performances of exhaust TiO_2 after 9 h of PFOA photodegradation were also evaluated by reusing it in an additional test performed on a standard 4 mM PFOA solution.

Photocatalysis follows the Langmuir–Hinshelwood model [25]. When the PFOA adsorption onto the photocatalyst surface is negligible, the reaction mechanism can be approximated to a pseudo-first order kinetic (1):

$$r = -\frac{dC}{dt} = k_{app}C \quad (1)$$

In Eq. (1), r is the reaction rate, C is the surfactant concentration in solution, t is the time and k_{app} is the apparent first order rate constant. The reactions were conducted without a constant feed of oxygen as reported by Li et al. [9], but using just the naturally dissolved O_2 (DO), in order to simulate conditions of non-enriched water, as industrially feasible.

2.3. X-ray photoelectron spectroscopy (XPS)

X-ray photoelectron spectroscopy analysis was performed to study the photocatalyst surface before and after the photodegradation reaction, in order to monitor composition variations that might have occurred. X-ray photoelectron spectroscopy spectra were obtained by using an M-probe apparatus (Surface Science Instruments). The source was monochromatic Al K_α radiation (1486.6 eV). A spot size of 200 μm × 750 μm and pass energy of 25 eV were used. 1 s level hydrocarbon-contaminant carbon was taken as the internal reference at 284.6 eV. Fittings were performed using pure Gaussian peaks, Shirley's baseline, and without any constraints. XPS analyses were conducted on samples obtained centrifuging and filtering through a 0.45 μm polycarbonate membrane the surfactant solution at different reaction times (2 h, 4 h, 9 h); the TiO_2 samples were then dried in inert atmosphere for 24 h and analyzed. Subsequently, in order to remove possible fluorinated organic compounds deposited on the catalyst surface, the samples were suspended in the fluorinated solvent $CF_3OCFClCF_2Cl$, dried in inert atmosphere and analyzed again.

For each sample, survey analyses in the whole range of X-ray spectra and high resolution analyses in the typical zone of C-1s, Ti-2p, O-1s and F-1s were performed.

2.4. High-performance liquid chromatography combined with mass spectrometry

Analytes separation was performed by using an Agilent 1100 Series HPLC Value System, consisting of a quaternary pump, vacuum degasser and autosampler. The instrument was equipped with a Lichrocart® 55-4 Purospher® STAR RP-18 endcapped column (55 × 4.0 mm i.d., 3 μm) supplied by Merck KGaA. For quantitative determination, the chromatographic system was interfaced to a Bruker Esquire 3000 Plus quadrupole ion trap mass spectrometer (Bruker Daltonics) operating in negative electrospray mode. Instrumental parameters were optimized to transmit the $[M-H]^-$ ion for all expected degradation intermediates. Primary ions monitored for PFOA, perfluoroheptanoic acid (PFHpA), perfluorohexanoic acid (PFHxA), perfluoropentanoic acid (PFPeA), perfluorobutanoic acid (PFBA), perfluoropropionic acid (PFPrA) and trifluoroacetic acid (TFA) determinations were 413, 363, 313, 263, 213, 163 and 113 m/z, respectively. Samples of the reaction mixture collected at different reaction times were diluted in deionized water (1:10) and injected in the HPLC–MS with 2 mM ammonium acetate/methanol as the mobile phase starting at 10% methanol. At a flow rate of 200 μL/min the gradient increased to 90% methanol at 5 min; before reverting to original conditions at 20 min, the gradient decreased to 80% methanol at 15 min. Column temperature was maintained at 40 °C.

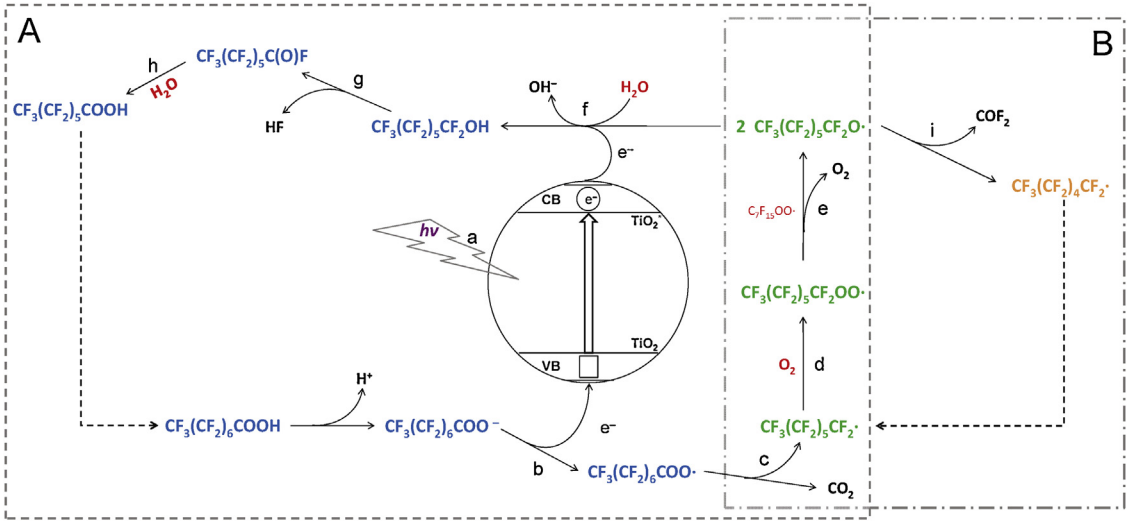

Fig. 1. Reaction mechanism of PFOA degradation in the presence of TiO_2 photocatalyst, comprehensive of both photo-redox (A) and b-scission (B) pathways.

2.5. Fluorine-19 nuclear magnetic resonance (^{19}F-NMR) spectroscopy

^{19}F-NMR experiments were performed on a Bruker 500 Ultrashield spectrometer operating at 470.30 MHz, in order to evaluate the trend of PFOA signals. In particular, samples of solution collected from the photoabatement reactor at the starting time (0 min), at 3 h and 9 h were analyzed by ^{19}F-NMR, using D_2O as deuterated solvent. PFOA integral calculation allowed the detection of degradation products by considering the ratio between CF_3, present in all the degradation by-products (C_2–C_7 perfluorinated acids) and CF_2 signals.

3. Results and discussion

3.1. Photocatalysis results

PFOA total degradation reaction in water can be summarized as follows:

$$CF_3(CF_2)_6COOH + 7/2O_2 + 7H_2O \rightarrow 8CO_2 + 15\,HF \quad (2)$$

The whole mechanism of PFOA decomposition in presence of TiO_2, comprehensive of both the photo-redox (Fig. 1A) and the β-scission (Fig. 1B) pathways, is presented in Fig. 1. The commonly accepted mechanism of PFOA decomposition starts with the excitation of titanium dioxide caused by the irradiation of UV light (Fig. 1—reaction a) [20,26]; excited TiO_2 accepts one electron from carboxylate of PFOA ($CF_3(CF_2)_6COO^-$) and a PFOA radical (Fig. 1—reaction b) is generated [7,20,26]. The so formed species undergoes a Kolbe decarboxylation reaction (Fig. 1—reaction c) [27,28]. The C_7 radical reacts with molecular oxygen present in the reaction environment and peroxyradicals are generated (Fig. 1—reaction d) [8]. The coupling of two peroxyradicals allows the formation of O_2 and two oxyradicals (Fig. 1—reaction e) that, in the presence of the surface excited electrons of TiO_2 and water, generate an unstable primary perfluorinated alcohol (Fig. 1—reaction f) [8,29]. This unstable compound originates acyl fluoride and hydrogen fluoride (Fig. 1—reaction g) [28,29,31]; in the presence of water, the acyl fluoride is hydrolyzed to the corresponding carboxylic acid C_{n-1}, $CF_3(CF_2)_5COOH$ (Fig. 1—reaction h) [28–31]. This photo-redox mechanism explains a step-by-step $C_n \rightarrow C_{n-1}$ chain length decrease of PFOA [8,28,32] and the formed carboxylic acid C_{n-1}, $CF_3(CF_2)_5COOH$, should compete with the PFOA on the catalytic sites of TiO_2 particles (Fig. 1—reaction b). Therefore, in the decomposition reaction the concentration of shorter chain perfluorinated acids should increase proportionally to fluoride formation according to pathway A in Fig. 1.

Another possible reaction pathway can be hypothesized assuming that the oxyradical formed in reaction (e) evolves eliminating COF_2 by mono molecular β-scission and consequent generation of a C_{n-1} radical (Fig. 1—reaction i in pathway B) [29,33–35]. The so formed carbon-centered perfluorinated radical takes part to reaction (d), while fluorophosgene is quenched in aqueous environment generating hydrogen fluoride and carbon dioxide [29]. Assuming that this pathway is active, it is remarkable that this mechanism can promote an almost complete PFOA decomposition without the formation of perfluorinated acids as intermediates. The key steps of the complete oxidation mechanism are represented by the two competing reactions: the bimolecular reduction of the oxyradical activated by TiO_2 surface (reaction f) and the monomolecular β-scission generating COF_2 and C_{n-1} radical (reaction i).

During the first 4 h of PFOA photoabatement, the major release of fluoride ions was recorded as a consequence of PFOA mineralization (Fig. 2A). This phenomenon might be promoted by a predominant β-scission mechanism, able to directly mineralize PFOA and to generate fluoride ions with negligible formation of shorter chain perfluorinated acids as degradation intermediates. The presence of fluoride ions in concentrations up to around 17 mM is reasonably related to the surface fluorination of TiO_2-catalyst. For the entire duration of the photoabatement process, it was possible to observe a decrease in the PFOA content in solution (Fig. 2B). Mineralization data obtained by TOC and IC determined that after 4 h of PFOA photoabatement the mineralization ratio was 32% and the yield in fluoride ions (calculated as the ratio of the concentration of fluoride ions over the initial concentration of PFOA multiplied by 15 due to the stoichiometric ratio) resulted to be 29% (Table S.I.1). The adsorption of fluoride ions on the surface of TiO_2 particles might be a reason of the fluoride ions loss (3%) in the aqueous phase.

The presence of an evident limit condition for the photomineralization (*plateau*) can be noticed in the kinetic curve after 4 h (Fig. 2A and B). In fact, the fluoride content and the percentage mineralization after 6 and 9 h remained equal to 29% and 32%, respectively. The lack of photoactivity of exhaust TiO_2 after 9 h of PFOA photodegradation was confirmed by evaluating its photocatalytic performances in a reusing test on a standard 4 mM PFOA solution: TOC data revealed that after additional 6 h PFOA mineralization was only 10% (Fig. S.I.1).

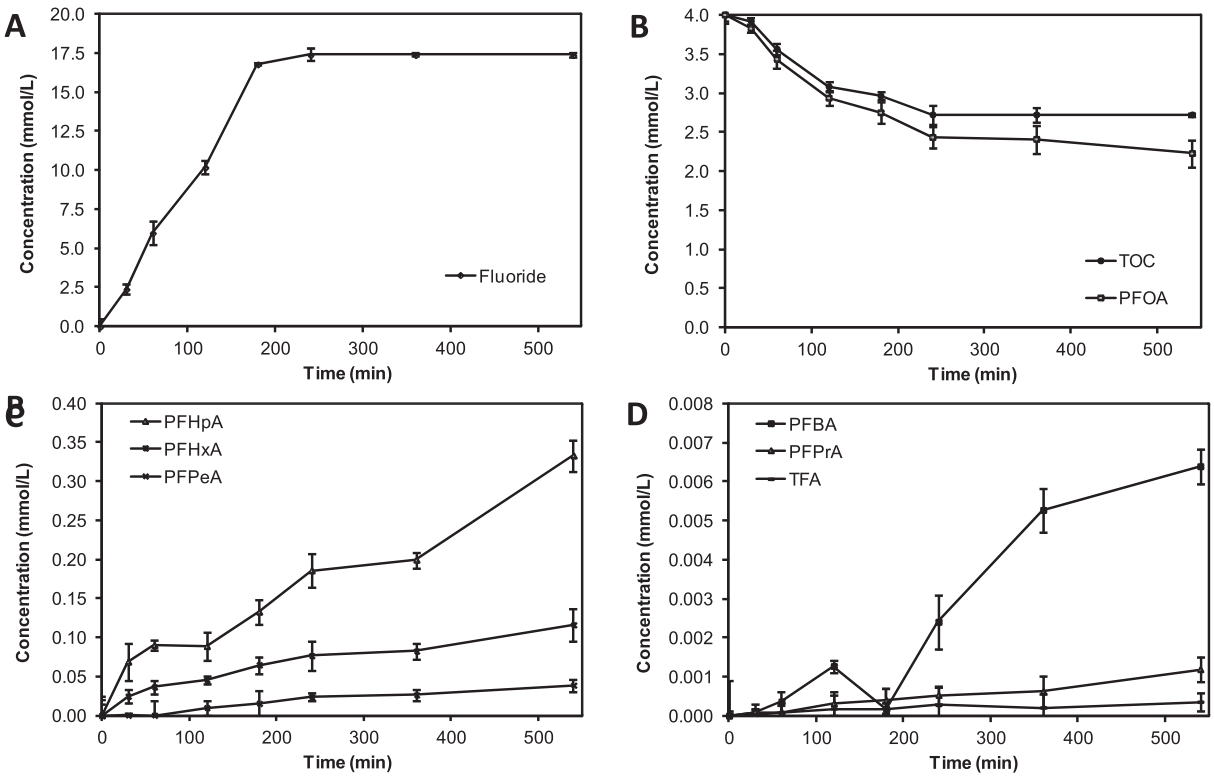

Fig. 2. Trends of fluoride ions release (A), total organic carbon content and PFOA concentration in solution (B), and degradation intermediates concentrations in solution ((C) and (D)).

In order to evaluate PFOA degradation intermediates content, samples of the solution from the photoabatement reactor were collected at different reaction times and analyzed by HPLC–MS (Table S.I.2). First, an increasing difference between the trends of TOC content and PFOA concentration was overall present and after 4 h it became particularly evident (Fig. 2B). However, even if the photoabatement rate of PFOA after 4 h was significantly reduced, an increase in the degradation intermediates concentrations was observed (Fig. 2C and D). The concentration trends of the degradation intermediates in solution followed a well-defined order: the higher the molecular weight of the intermediate, the higher its presence in solution (PFHpA > PFHxA > PFPeA > PFBA > PFPrA > TFA). However, all the expected degradation intermediates were already detected in the sample collected after 30 min, even if their presence in solution was negligible if compared to PFOA conversion and fluoride formation (Fig. 2A–D). It is important to notice that the shorter chain acids formation during PFOA decomposition is not sufficient to explain the fluoride evolution observed and shown in Fig. 2A and C. This gives further prove of the coexistence of two PFOA decomposition pathways, as shown in Fig. 1.

In addition, the presence in solution of TFA and PFPrA after 30 min of treatment (Fig. 2D) could not be ascribed to photo-redox $C_n \rightarrow C_{n-1}$ chain length decrease mechanism, but it could be justified by a competitive direct chain length decomposition mechanism based on the elimination of COF_2 as decomposition product induced by β-scission reactions of the oxyradical formed in reaction (e) (Fig. 1). The photo-redox $C_n \rightarrow C_{n-1}$ chain length decrease mechanism appeared to be significant after 4 h of photoabatement, when the mineralization rate of PFOA was evidently lowered.

Kinetic data of photodegradation of a 4 mM PFOA solution revealed that, under an UV irradiation of 95 W/m^2 and with a TiO_2 content of 0.66 g/L, the degradation fitted with a pseudo-first order kinetic during the first 4 h (Fig. 3). The kinetic apparent constant (k_{app}) referring to the rate of PFOA disappearance was equal to 0.1296 h^{-1} (R^2 = 0.9956).

As reported in the literature, no PFOA abatement was observed working in the presence of TiO_2 as photocatalyst without UV irradiation as well as under UV irradiation in the absence of photocatalyst (photolysis) [24].

In order to understand the chemical modification induced on TiO_2 photocatalyst during the degradation process, the high-resolution XPS spectra in the F-1s region were recorded on TiO_2 samples collected at different reaction times. After 2 and 4 h of photodegradation (Fig. 4A and B), XPS analysis revealed two peaks at around 684 and 688 eV which can be attributed to molecules of hydrofluoric acid and PFOA, respectively, adsorbed on the TiO_2 surface. After 9 h the XPS spectrum in the F-1s region showed three peaks which could be assigned to different fluorinated species (Fig. 4C): the first peak at around 684 was still related to adsorbed hydrofluoric acid; the signal at around 687 eV was due to the formation of fluorinated $TiO_{(2-x/2)}F_x$ species induced by fluoride ions generated during the photoabatement of PFOA [36]; the third peak at around 690 eV could be assigned to fluorinated organic derivatives generated during the PFOA photodegradation and adsorbed on the photocatalyst surface. Further evidences of fluoride adsorption on the surface of TiO_2 particles were derived from the difference between the mineralization ratio and the yield in fluoride ions (3% after 4 h) as well as from a mass balance of fluorine atoms. Mass balances of fluorine atoms at different reaction times have been evaluated on the basis of the concentrations of initial PFOA, residual PFOA, degradation intermediates (PFHpA, PFHxA, PFPeA, PFBA, PFPrA, TFA) and fluoride ions (Table S.I.2). The results of mass balance calculation revealed an increasing loss of fluorine, till about 5% loss of fluorine after 9 h. The incorporation of a moderate amount of fluoride ions as dopant onto TiO_2 nanoparticles generally enhances effectively their photocatalytic activity due

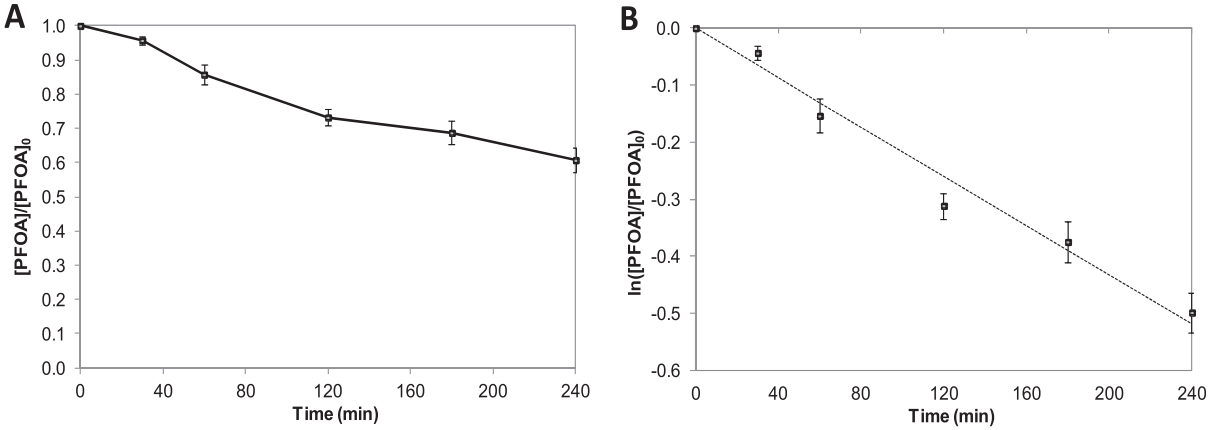

Fig. 3. PFOA photodegradation kinetic data plotted against time as [PFOA]/[PFOA]0 (A) and its corresponding linearization (B).

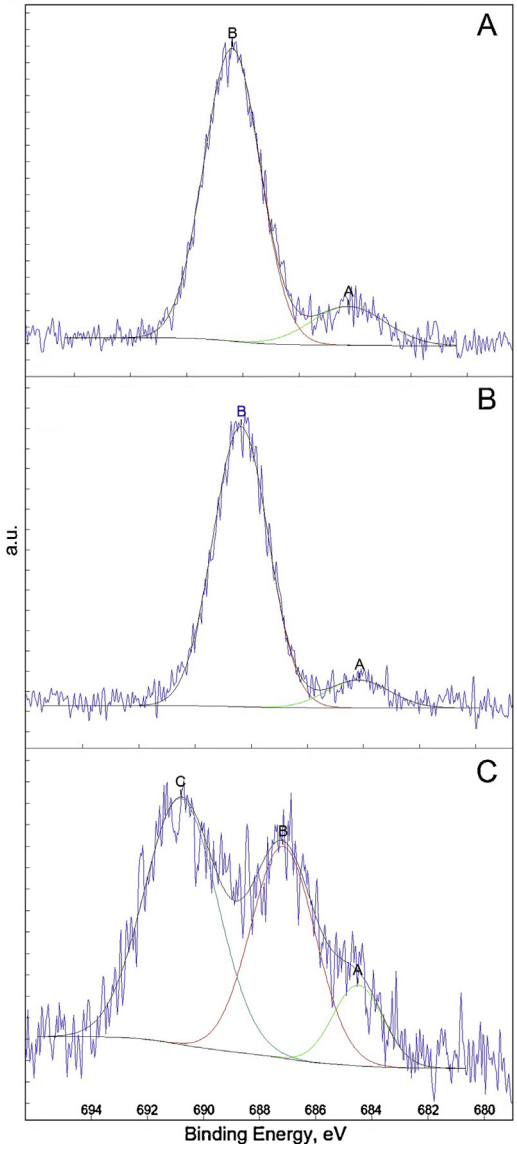

Fig. 4. XPS results—F-1s region XPS spectra of titanium dioxide catalyst: after 2 h (A); after 4 h (B); after 9 h reaction (C).

to the formation of Ti–F species on the facets [37–48]. However, variations of reaction operative conditions, especially pH, and use of an excessive F:Ti molar ratio can cause an opposite behavior: the stabilization of F^- ions in the vicinity of Ti^{4+} cations and the limitation of charge carriers mobility hinder the photocatalytic activity of TiO_2 [36]. These results were in agreement with the XPS analyses in the Ti-2p region recorded on catalyst samples collected at different reaction times: in the first 4 h of photoabatement, no variations were observed on the TiO_2 surface and both binding energy values and peaks distribution remained almost identical to that of the pristine P25; conversely, considerable variations were noticed after 9 h of PFOA photodegradation [24].

The assignments of ^{19}F-NMR spectra of PFOA (Fig. S.I.2), referring to the labeled formula $CF_{3(m)}CF_{2(n)}CF_{2(o)}CF_{2(p)}CF_{2(q)}CF_{2(r)}CF_{2(s)}COOH$, were in agreement with literature: δ = −81.4 (3 F, F_m), −126.7 (2 F, F_n), −123.7 (2 F, F_o), −123.4 (2 F, F_p), −122.6 (2 F, F_q), −122.4 (2 F, F_r), −117.9 (2 F, F_s) ppm [49]. The presence of the same set of 7 signals in both the starting and the final solutions suggested that a significant portion of undecomposed PFOA remained. Only at the end of the considered decomposition time (9 h), the amount of shorter acids in solution was enough to be clearly detected and a peak due to a CF_2 near a CF_3 not ascribable to PFOA appeared at −131 ppm (Fig. S.I.3) [50]. Peaks of shorter perfluorinated acids have almost the same chemical shifts of the corresponding signals of PFOA [49–51]. The integrals of the signals in the ^{19}F-NMR spectra recorded at 0 min, 3 h and 9 h were also calculated (Fig. S.I.2–4). The $CF_{3(m)}$ integral was used as reference, with an imposed value of 3. The PFOA mineralization results in less concentrated solutions of the starting acid and, consequently, the ratio between ^{19}F-NMR integrals of $CF_{3(m)}$ and of all the CF_2 should remain constant. If PFOA decomposition stops before the complete mineralization, shorter perfluorinated acids should be generated. In this situation, the elimination of COF_2 in pathway B (Fig. 1—reaction i) as well as the decarboxylation in pathway A (Fig. 1—reaction c) reduce the number of CF_2 groups in the chains and, consequently, the number of peaks in ^{19}F-NMR spectra. In the starting solution (0 min), the ratio between CF_3 and CF_2 integrals was 3:2 (Fig. 5). After 3 h, the integrals of two inner CF_2 signals, $CF_{2(p)}$ and $CF_{2(q)}$, slightly decreased, because of the formation of perfluorinated acids with shorter chains. In fact, these acids have progressively a lower number of CF_2 groups than PFOA and a CF_3 as carbon-chain end-group. Therefore, a diminishing number of CF_2 signals can contribute to the ^{19}F-NMR spectra even if the CF_3 signal is present until the complete mineralization of PFOA. After 9 h, the relative integral of four CF_2 signals, $CF_{2(n)}$, $CF_{2(p)}$, $CF_{2(q)}$ and $CF_{2(r)}$,

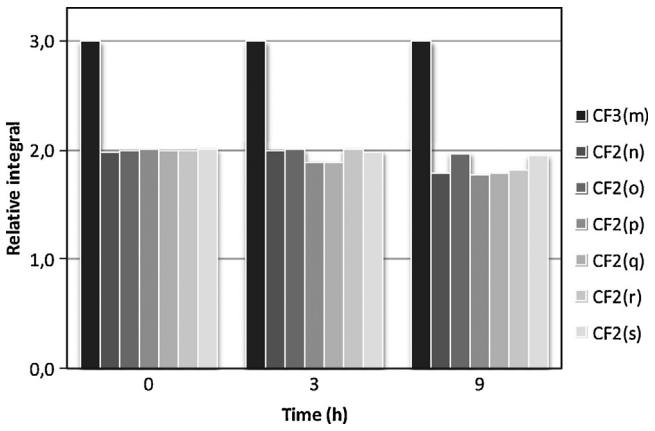

Fig. 5. ^{19}F-NMR spectra integrals values at different decomposition time. All the CF_2 integral values are relative to their ratio with CF_3 ones and the assignments are referred to the labeled formula of PFOA: $CF_3(m)CF_2(n)CF_2(o)CF_2(p)CF_2(q)CF_2(r)CF_2(s)COOH$.

decreased and this can be due to the formation of perfluorinated acids with even shorter chains.

4. Conclusions

The influence of fluoride ions on the surface of titanium dioxide, during the perfluorooctanoic acid degradation, was studied. The photocatalytic reaction was carried out working under optimal conditions, using a 4 mM PFOA solution and a TiO_2 content of 0.66 g/L under a UV irradiation of 95 W/m^2. The degradation mechanism was investigated by HPLC–MS analysis, confirming the presence of the intermediates through two possible degradation pathways: the photo-redox and the β-scission pathway. The mechanism based on β-scission reactions resulted dominant during the first 4 h of photoabatement, when the complete mineralization with the fastest rate of fluoride release is more significant; afterwards, the photo-redox mechanism prevailed and noticeable concentrations of shorter chain perfluorinated acids as degradation intermediates were observed. The PFOA concentration was monitored during the reaction and a kinetic apparent constant (k_{app}) referring to the rate of PFOA disappearance was measured as equal to 0.1296 h^{-1}. The surface of TiO_2 was analyzed by XPS technique, revealing the modification of TiO_2 catalyst after 9 h of reaction. The surface modification was induced by fluoride ions due to hydrofluoric acid generated by PFOA degradation and it might influence the catalyst reducing the photocatalytic efficiency of TiO_2. ^{19}F-NMR analysis revealed the signals due to PFOA in both the starting and the final solutions, proving that the surfactant was not completely decomposed.

Acknowledgements

The authors wish to acknowledge with thanks the generous support and the valuable interactions induced to this research in the field of fluorinated materials by the institution of the Politecnico di Milano/Solvay Fluorine Chemistry Chair. This work has been supported by MIUR (PRIN 2010-2011).

Appendix A. Supplementary data

Supplementary data associated with this article can be found, in the online version, at http://dx.doi.org/10.1016/j.cattod.2014.04.031.

References

[1] M.M. Schultz, D.F. Barofsky, J.A. Field, Environ. Eng. Sci. 20 (5) (2003) 487–501.
[2] I.T. Cousins, R.C. Buck, S.H. Korzeniowski, Environ. Sci. Technol. 40 (2006) 32–44.
[3] M. Ylinen, H. Hanhijärvi, P. Peura, O. Rämö, Arch. Environ. Contam. Toxicol. 14 (1985) 713–717.
[4] F. Persico, M. Sansotera, M.V. Diamanti, L. Magagnin, F. Venturini, W. Navarrini, Thin Solid Films 545 (2014) 210–216.
[5] D.M. Lemal, J. Org. Chem. 69 (2004) 1–11.
[6] H. Hori, E. Hayakawa, H. Einaga, S. Kutsuna, K. Koike, T. Ibusuki, H. Kiatagawa, R. Arakawa, Environ. Sci. Technol. 38 (2004) 6118–6124.
[7] A. Zaggia, B. Ameduri, Curr. Opin. Colloid Interface Sci. 17 (2012) 188–195.
[8] H. Lin, J. Niu, S. Ding, L. Zhang, Water Res. 46 (2012) 2281–2289.
[9] X. Li, P. Zhang, L. Jin, T. Shao, Z. Li, J. Cao, Environ. Sci. Technol. 46 (2012) 5528–5534.
[10] US EPA, Revised Draft—Hazard Assessment of Perfluorooctanoic Acid and Its Salts, Office of Pollution Prevention and Toxics, Risk Assessment Division, 2002 (November 4, 2002).
[11] U. Järnberg, K. Holmström, B. van Bavel, A. Kärrman, Perfluoroalkylated acids and related compounds (PFAS) in the Swedish environment—Chemistry, Sources & Exposure, in: Report to Swedish Environment Protection Agency, 2006.
[12] M. Cheryan, N. Rajagopalan, J. Membr. Sci. 151 (1998) 13–28.
[13] H. Yoo, J.W. Washington, T.M. Jenkins, E.L. Libelo, J. Chromatogr. A 1216 (2009) 7831–7839.
[14] E.L. Hawley, P.E. Tessa Pancras, M.S. Jeffrey Burdick, An ARCADIS White Paper, 2012, pp. 1–9.
[15] C. Flores, F. Ventura, J. Martin-Alonso, J. Caixach, Sci. Total Environ. 461–462 (2013) 618–626.
[16] C.D. Vecitis, H. Park, J. Cheng, B.T. Mader, M.R. Hoffmann, Environ. Sci. Eng. Chin. 3 (2) (2009) 129–151.
[17] H. Lutze, S. Panglisch, A. Bergmann, T.C. Schmidt, Treatment options for the removal and degradation of polyfluorinated chemicals, in: T.P. Knepper, F.T. Lange (Eds.), Polyfluorinated Chemicals and Transformation Products, Hdb. Env. Chem., Springer, Heidelberg, 2012, pp. 103–125.
[18] A. Mills, N. Elliott, I.P. Parkin, S.A. O'Neill, R.J. Clarke, J. Photochem. Photobiol., A: Chem. 151 (2002) 171–179.
[19] A. Mills, S. Le Hunte, J. Photochem. Photobiol., A: Chem. 108 (1997) 1–35.
[20] R. Munter, Proc. Est. Acad. Sci. Chem. 50 (2001) 59–80.
[21] W. Navarrini, M.V. Diamanti, M. Sansotera, F. Persico, M. Wu, L. Magagnin, S. Radice, Prog. Org. Coat. 74 (2012) 794–800.
[22] C.L. Bianchi, S. Gatto, C. Pirola, A. Naldoni, A. Di Michele, G. Cerrato, V. Crocellà, V. Capucci, Appl. Catal., B: Environ. 146 (2014) 123–130.
[23] T. Ohno, K. Sarukawa, K. Tokieda, M. Matsumura, J. Catal. 203 (2001) 82–86.
[24] M. Sansotera, F. Persico, C. Pirola, W. Navarrini, A. Di Michele, C.L. Bianchi, Appl. Catal., B: Environ. 148 (2014) 29–35.
[25] E. Selli, C.L. Bianchi, C. Pirola, G. Cappelletti, J. Hazard. Mater. 153 (2008) 1136–1141.
[26] O. Carp, C.L. Huisman, A. Reller, Prog. Solid State Chem. 32 (2004) 33–177.
[27] S.C. Panchangam, A.Y.C. Lin, J.H. Tsai, C.F. Lin, Chemosphere 75 (2009) 654–660.
[28] Y. Wang, P. Zhang, J. Hazard. Mater. 192 (2011) 1869–1875.
[29] S. Kutsuna, H. Hori, Int. J. Chem. Kinet. 39 (2007) 276–288.
[30] C. Kormann, D.W. Bahnemann, M.R. Hoffmann, Environ. Sci. Technol. 25 (1991) 494–500.
[31] S. Talaeemashhadi, M. Sansotera, C. Gambarotti, A. Famulari, C.L. Bianchi, P.A. Guarda, W. Navarrini, Carbon 59 (2013) 150–159.
[32] W.J. De Bruyn, J.A. Shorter, P. Davidovits, D.R. Worsnop, M.S. Zahniser, C.E. Kolb, Environ. Sci. Technol. 29 (1995) 1179–1185.
[33] M. Sansotera, W. Navarrini, M. Gola, C.L. Bianchi, P. Wormald, A. Famulari, M. Avataneo, J. Fluorine Chem. 132 (2011) 1254–1261.
[34] A.M.B. Giessing, A. Feilberg, T.E. Mögelberg, J. Sehested, M. Bilde, T.J. Wallington, O.J. Nielsen, J. Phys. Chem. 100 (1996) 6572–6579.
[35] M. Sansotera, W. Navarrini, L. Magagnin, C.L. Bianchi, A. Sanguineti, P. Metrangolo, G. Resnati, J. Mater. Chem. 20 (2010) 8607–8616.
[36] A. Demourgues, N. Penin, E. Durand, F. Weill, D. Dambournet, N. Viadere, A. Tressaud, Chem. Mater. 21 (2009) 1275–1283.
[37] Q. Wang, C. Chen, D. Zhao, W. Ma, J. Zhao, Langmuir 24 (2008) 7338–7345.
[38] S. Liu, J. Yu, B. Cheng, M. Jaroniec, Adv. Colloid Interface Sci. 173 (2012) 35–53.
[39] G. Liu, C. Sun, H.G. Yang, S.C. Smith, L. Wang, G.Q.M. Lu, H.-M. Cheng, Chem. Commun. 46 (2010) 755–757.
[40] W. Ho, J.C. Yu, S. Lee, Chem. Commun. 10 (2006) 1115–1117.
[41] H. Zhang, P. Liu, F. Li, H. Liu, Y. Wang, S. Zhang, M. Guo, H. Cheng, H. Zhao, Chem.-Eur. J. 17 (2011) 5949–5957.
[42] D. Zhang, G. Li, X. Yang, G.C. Yu, Chem. Commun. 29 (2009) 4381–4383.
[43] G. Wu, J. Wang, D.F. Thomas, A. Chen, Langmuir 24 (2008) 3503–3509.
[44] M. Liu, L. Piao, L. Zhao, S. Ju, Z. Yan, T. He, C. Zhou, W. Wang, Chem. Commun. 46 (2010) 1664–1666.
[45] X. Han, Q. Kuang, M. Jin, Z. Xie, L. Zheng, J. Am. Chem. Soc. 131 (2009) 3152–3153.

[46] H.G. Yang, G. Liu, S.Z. Qiao, C.H. Sun, Y.G. Jin, S.C. Smith, J. Zou, H.M. Cheng, G.Q.M. Lu, J. Am. Chem. Soc. 131 (2009) 4078–4083.
[47] D. Li, H. Haneda, N.K. Labhsetwar, S. Hishita, N. Ohashi, Chem. Phys. Lett. 401 (2005) 579–584.
[48] J. C: Yu, J. Yu, W. Ho, Z. Jiang, L. Zhang, Chem. Mater. 14 (2002) 3808–3816.
[49] A.H. Karoyo, A.S. Borisov, L.D. Wilson, P. Hazendonk, J. Phys. Chem. B 115 (2011) 9511–9527.
[50] A.A. Ribeiro, J. Fluorine Chem. 83 (1997) 61–66.
[51] W.R. Dolbier, Guide to Fluorine NMR for Organic Chemists, Wiley, Hoboken, 2009.